8-1-2012

Node Filtering and Face Routing for Sensor Network

Umang Amatya
University of Nevada, Las Vegas, umangama@hotmail.com

NODE FILTERING AND FACE ROUTING FOR SENSOR NETWORK

by

Umang Amatya

Bachelor of Computer Engineering, I.O.E., Pulchowk Campus

Tribhuvan University, Nepal

2007

A thesis submitted in partial fulfillment

of the requirements for the

Master of Science in Computer Science

Department of Computer Science

Howard R. Hughes College of Engineering

The Graduate College

University of Nevada, Las Vegas

August 2012

THE GRADUATE COLLEGE

We recommend the thesis prepared under our supervision by

Umang Amatya

entitled

Node Filtering and Face Routing for Sensor Network

be accepted in partial fulfillment of the requirements for the degree of

Master of Science in Computer Science
Department of Computer Science

Laxmi P. Gewali, Committee Chair

John T. Minor, Committee Member

Juyeon Jo, Committee Member

Rama Venkat, Graduate College Representative

Thomas Piechota, Ph. D., Interim Vice President for Research and Graduate Studies and Dean of the Graduate College

August 2012

ABSTRACT

Node Filtering and Face Routing for Sensor Network

by

Umang Amatya

Dr. Laxmi P. Gewali, Examination Committee Chair

Professor of Computer Science

University of Nevada, Las Vegas

Greedy forward routing and face routing algorithms have been extensively used for sending messages in sensor networks. In this thesis, we consider the problem of filtering redundant nodes in a sensor network as a pre-processing step for face routing. We propose two algorithms for identifying redundant nodes. We test the performance of proposed filtering algorithms on generated networks. The prototype algorithm for testing the proposed algorithms has been implemented in the Java programming language. Experimental investigation shows that the proposed filtering algorithms are effective in removing redundant nodes without compromising the network connectivity.

ACKNOWLEDGEMENTS

I would like to express my sincere gratitude to my advisor Dr. Laxmi P. Gewali for the continuous support of my thesis, for his patience, motivation, enthusiasm, and immense knowledge. His guidance helped me a lot during my thesis. I feel that I am very lucky to have an advisor like him. I would also like to thank Dr. John T. Minor, Dr. Ju-Yeon Jo and Dr. Rama Venkat for serving as committee members.

I would also like to thank my friends: Bishal, Dinesh, Kishor dai, Krishna, Pinthep and Romas for their help and support.

Last but not least, I would like to thank my dad and my mom for their love and blessing.

TABLE OF CONTENTS

ABSTRACT iii

ACKNOWLEDGEMENTS iv

LIST OF FIGURES vii

LIST OF TABLES ix

CHAPTER 1 INTRODUCTION 1

CHAPTER 2 REVIEW 4

2.1 Gabriel graphs 4

2.1.1 Algorithm to implement Gabriel graphs 5

2.2 Relative neighborhood graph 7

2.2.1 Algorithm to implement Relative neighborhood graph 7

2.3 Delaunay Triangulation and Variations 8

2.3.1 Restricted Delaunay Graph(RDG) 10

2.4 Routing 11

2.4.1 Greedy forward routing 12

2.4.2 Face routing 13

2.4.3 Hybrid greedy face routing 14

CHAPTER 3 NODE FILTERING FOR FACE ROUTING 16

3.1 Compressing Equivalent Nodes 16

3.2 Solo-Faced Chains 19

3.3 Extracting Biconnected Clusters 24

3.3.1 Planar Graph 24

3.3.2 Planar Straight Line Graph 24

3.3.3 Doubly Connected Edge List (DCEL) 24

3.3.4 Degree of Vertices 26

3.3.5 Removal of Floating Chains 26

CHAPTER 4 IMPLEMENTATION 32

4.1 Introduction to Java 32
4.2 Interface Description 33
4.2.1 Project 1 33
4.2.2 Project 2 35
4.2.3 Project 3 39
4.3 Observation 41
CHAPTER 5 CONCLUSION 45
REFERENCES 47
VITA 49

LIST OF FIGURES

Figure 2.1 Formation of Gabriel graph for five point sites 4
Figure 2.2 Formation of relative neighborhood graph of five point sites . . . 7
Figure 2.3 Illustrating empty lune of influence test 8
Figure 2.4 Illustrating Delaunay Triangulation 8
Figure 2.5 Illustrating Empty Circle in Delaunay Triangulation 9
Figure 2.6 Illustrating formation of restricted delaunay graph 11
Figure 2.7 Illustrating Greedy routing 12
Figure 2.8 Illustrating Face Routing 13
Figure 2.9 Illustrating Hybrid greedy face routing 14

Figure 3.1 Illustrating Equivalent nodes p_5 and p_6 16
Figure 3.2 Illustrating Clusters of Equivalent nodes 17
Figure 3.3 Illustrating Gabriel Graph and its compressed version 18
Figure 3.4 Illustrating a Proof of Lemma 3.1.1 18
Figure 3.5 Gabriel graph showing edges and its equivalent half edge 19
Figure 3.6 Illustrating Solo-Faced Chains 20
Figure 3.7 Illustrating Bridge Solo-Faced Chain (ch_3-drawn dashed) 21
Figure 3.8 Illustrating clusters of nodes connected by Bridge Solo-Faced Chains 22
Figure 3.9 Tree representation of Bridge Solo-Faced Chains 22
Figure 3.10 Illustrating cluster of nodes without Non Bridge Solo-Faced Chains 23
Figure 3.11 Illustrating cluster of nodes after removing External-Components and External Solo-Faced Chains 23
Figure 3.12 Illustrating Planar Straight Line Graph (PSLG) 24
Figure 3.13 Illustrating Doubly Connected Edge List data structure 25
Figure 3.14 Graph showing edges and its equivalent half edge 27
Figure 3.15 Graph showing floating chains. 28
Figure 3.16 Illustrating biconnected graph 29
Figure 3.17 Illustrating biconnected components and bridge chains 29
Figure 3.18 DCEL representation of biconnected components and bridge chains 29
Figure 3.19 Illustrating transition half-edge 30

Figure 4.1 Illustrating User Interface of Project 1 33
Figure 4.2 Illustrating Random Nodes 34
Figure 4.3 Illustrating Gabriel Graph containing source and target nodes . 35
Figure 4.4 Illustrating the routing path taken from source node to target node 36
Figure 4.5 Illustrating the user interface of Project 2 36
Figure 4.6 Illustrating solo-faced chains 37
Figure 4.7 Illustrating graph containing external segments 37
Figure 4.8 Illustrating graph after removal of external segments 38
Figure 4.9 Illustrating equivalent nodes 38

Figure 4.10 Illustrating user interface of project 3 39
Figure 4.11 Illustrating greedy routing traced by nodes 40
Figure 4.12 Illustrating face routing traced by nodes 40

LIST OF TABLES

Table 3.1 Record for each half-edge 25
Table 3.2 Record for each face 26
Table 3.3 Record for each Vertex 26

Table 4.1 Nodes and their range 41
Table 4.2 Total changes in equivalent nodes 42
Table 4.3 Total changes in hubs (partially connected graph) 43
Table 4.4 Total changes in hubs (completely connected graph) 44

CHAPTER 1

INTRODUCTION

Development of efficient algorithms and protocols for sensor network application has attracted the interest of many researchers for the last 10 years [6]. Sensor networks have been applied to solve problems in many areas of science and engineering that include robotics, emergency response, environmental monitoring, remote sensing, manufacturing, and law enforcement [16]. A sensor network is formed by wirelessly connecting sensor nodes which are distributed on a two dimensional surface or embedded in some equipment or gadgets. A sensor node is essentially a small electrical device containing (i) a small amount of memory, (ii) a low capacity processing unit, (iii) a radio communication component with range 300 meters, and (iv) some sensing components for measuring physical quantities such as temperature, pressure, humidity, etc. Nodes within the transmission range can exchange information wirelessly. Nodes outside the transmission range can communicate by establishing a sequence of in-range intermediate nodes between them. This kind of establishing in-range intermediate nodes between two distinct nodes is called *routing*.

Computation in a sensor network is much different than in a traditional wired network. In a sensor network, there is no centralized control for communication. Communication and computation is preferred to be done locally in a distributed manner. Each node only knows the position of itself and its in-range neighbors. A node can explore the presence of other nearby nodes by exchanging information between k-hop neighbors, where k is usually 1,2, or 3. Computing global properties of the sensor network that include connectivity, clustering, and coverage by exploring upto k-hop neighbors (for small k) are the most challenging problems in this emerging

area of computer science and engineering. Some good progress has been made for performing routing and clustering in recent years [9] and there are a wealth of fertile problems to pursue further research.

In this thesis, we are mainly concerned about filtering of nodes as a pre-processing step for routing in sensor networks. We basically try to identify redundant nodes present on a network so that we can eliminate such nodes and make the routing algorithms and protocols more effective and efficient.

Chapter two presents a review of planar graphs that includes Gabriel graph (gg), relative neighborhood graph (rng), Delaunay triangulation (dt), and restricted Delaunay graph (rdg). This chapter also contains a review of routing algorithms from computational geometry that includes greedy forward, face routing, and hybrid greedy face routing.

The main contributions of the thesis are in Chapter 3. It contains algorithms for filtering nodes as preprocessing for Face routing. We start with the formulation of the concepts "redundant nodes" and "equivalent nodes". The proposed filtering algorithms are based on retaining only one member from a set of identified redundant nodes. We show how the removal of a node from a pair of equivalent nodes does not alter the connectivity and routing construction.

Chapter four describes the implementation of algorithms for generating planar networks and algorithms for routing that include greedy routing, face routing, and hybrid greedy face routing. These algorithms are implemented in Java programming language. The implementation has a front-end graphical user interface that makes it easy to execute algorithms for generating planar networks and for constructing routing. Chapter four also contains results of the experimental investigation of the performance of face routing algorithms after applying filtering. The results show that the quality of generated routes are preserved after filtering.

In chapter five, we describe the performance of proposed algorithms for several

input node distributions. We also suggest some problems for future research.

CHAPTER 2

REVIEW

In this chapter, we present a comprehensive review of networks that are used for communication and routing in sensor networks. Most networks reviewed in this chapter are locally computable, which include Gabriel graph (GG), relative neighborhood graph (RNG), restricted Delaunay graph (RDG), and Delaunay triangulation (DT).

2.1 Gabriel graphs

A Gabriel graph GG(S) of a set of point sites S = $\{p_0, p_1, p_2, \ldots, p_{n-1}\}$ is a network structure first introduced by Gabriel and Sokal [8] in 1969 for analyzing geographic variation in zoology [10]. This structure is now extensively used for routing in sensor network and related applications. Gabriel graphs are used to model proximity (nearness) relations between nodes in two dimensional surfaces.

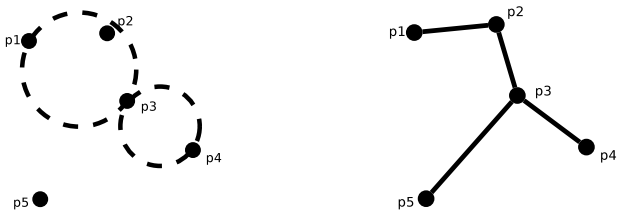

(a) Point sites S (b) Gabriel graph

Figure 2.1: Formation of Gabriel graph for five point sites

Formally, given a set of point sites S = $\{p_0, p_1, p_2, \ldots, p_{n-1}\}$, two point sites p_i and p_j are connected by an edge $e_{i,j}$ if the disk with diameter ending at p_i and p_j does not contain any other point sites. Figure 2.1 illustrates the formation of a Gabriel graph for five point sites. As shown in Figure 2.1a, the disk with diameter $<p_3,p_4>$ is empty and hence p_3 and p_4 is connected by an edge. On the other hand, the disk

with diameter $<p_1,p_3>$ is not empty and hence they are not connected by an edge. The Gabriel graph constructed in this manner is shown in Figure 2.1b.

For applications in sensor networks, only those point sites p_i and p_j are considered for possible edge connection if the distance between them is less or equal to the wireless transmission range of nodes.

2.1.1 Algorithm to implement Gabriel graphs

Given a set of point sites S = $\{p_0, p_1, p_2, \ldots, p_{n-1}\}$, perform empty circle tests for each pair of points by creating a circle with diameter p_i and p_j and checking if other points lie inside it or not. If the circle is empty, then connect those two points. The graph obtained in this manner is a Gabriel graph. Here, C_2^n pair of circles has to be checked for emptiness with n other points. Hence, the total time complexity of this algorithm is O(n^3). This algorithm can be called a *Brute Force Algorithm*.

Since a Gabriel graph is a subset of Delaunay triangulation, we can construct Gabriel graphs using Delaunay triangulation. First of all, find Delaunay triangulation of point sites. This can be computed in O($nlogn$) time. Then, perform empty circle tests on the edges of Delaunay triangle and remove the edges that contain other points inside them. Here the circle considered for empty test is the circle with the candidate Delaunay edge as the diameter. Since the edges of Delaunay triangle are of order n and we need to check for emptiness with n other points, the total time complexity of this algorithm is O(n^2). Such an algorithm can be called a Delaunay Guided Empty Circle algorithm.

There is another more efficient algorithm to compute Gabriel graphs where we don't need to perform any empty circle tests [10], which can be named a Delaunay and Voronoi Guided Algorithm. We can use the concept of Delaunay triangulation and Voronoi diagram to construct it. Every edge of Delaunay triangle has its dual Voronoi edge. The edge belongs to the Gabriel graph if and only if the edge of

Delaunay triangle intersects its dual Voronoi edge. It takes O($nlogn$) time to compute both Delaunay triangulation and Voronoi diagram and since all edges are of order n, it takes O(n) time to check for intersection. Thus the total time complexity of this algorithm is O($nlogn$).

The formal sketch of these three algorithms are given below:

Algorithm 1 Basic Algorithm (Brute Force)

```
1: for i = 0 to TotalVertices − 1 do
2:    for j = 0 to TotalVertices − 1 do
3:       p1 ← Vertices[i]
4:       p2 ← Vertices[j]
5:       if circle containing p1 and p2 as diameter is empty then
6:          connect p1 and p2
7:       end if
8:    end for
9: end for
```

Algorithm 2 (Delaunay Guided Empty Circle Algorithm)

```
1: Find delaunay triangulation induced by point sites in S
2: for i = 0 to TotalDelaunayEdges − 1 do
3:    p1 ← DelaunayEdge[i].source
4:    p2 ← DelaunayEdge[i].target
5:    if circle containing p1 and p2 as diameter is empty then
6:       connect p1 and p2
7:    end if
8: end for
```

Algorithm 3 (Delaunay and Voronoi Guided Algorithm)

```
1: Find voronoi diagram induced by point sites in S
2: Find delaunay triangulation induced by point sites in S
3: for i = 0 to TotalDelaunayedges − 1 do
4:    if DelaunayEdges[i] intersect DelaunayEdges[i].dual then
5:       print DelaunayEdges[i]
6:    end if
7: end for
```

2.2 Relative neighborhood graph

The relative neighborhood graph was proposed by Godfried Toussaint in 1980 [15] as a way of defining a structure from a set of points that would match human perceptions of the shape of the set. This graph is also used to model proximity (nearness) relations between nodes in two dimensional space.

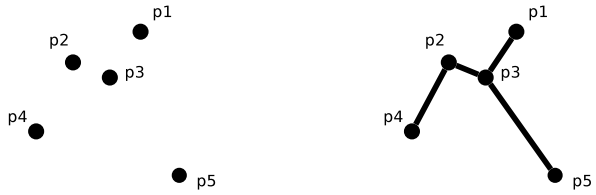

(a) Point Sites S (b) RNG

Figure 2.2: Formation of relative neighborhood graph of five point sites

Given a set of point sites S= $\{p_0, p_1, p_2, \ldots, p_{n-1}\}$, two point sites p_i and p_j are connected if and only if there does not exist a third point p_k that is closer to both p_i and p_j than they are to each other. Figure 2.2 shows the relative neighborhood graph for the set of five point sites. Here, p_1 and p_3 are connected by an edge because there are no two edges $<p_1,p_k>$ and $<p_3,p_k>$ which are shorter than the edge $<p_1,p_3>$. On the other hand, point sites p_1 and p_2 are not connected because there are two edges $<p_1,p_3>$ and $<p_2,p_3>$ which are shorter than $<p_1,p_2>$.

For applications in sensor networks, we consider the transmission range of point sites and connect only those two point sites that are within transmission range.

An alternative definition of RNG can be given as follows. Two points p_i and p_j are defined as relatively close to each other if $d(p_i,p_j) \leq max[d(p_i,p_k), d(p_j,p_k)]$ for all $k=1...n$ and $k \neq i,j$. The graph thus obtained by connecting only points p_i and p_j that are relative neighbors is the relative neighborhood graph.

2.2.1 Algorithm to implement Relative neighborhood graph

Given a set of point sites S= $\{p_0, p_1, p_2, \ldots, p_{n-1}\}$, perform empty lune of influence tests for each pair of points by creating a circle with center at p_i and p_j and

radius equal to $<p_i,p_j>$ and checking if other points lie inside the lune or not. If the lune is empty, then connect those two points. The graph obtained in this manner is a relative neighborhood graph. Here, C_2^n lunes have to be checked for emptiness with n other points. Hence, the total time complexity of this algorithm is $O(n^3)$.

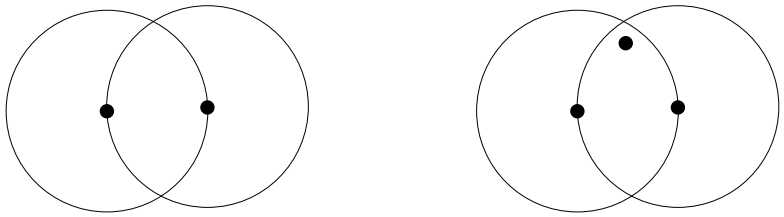

(a) empty lune (b) non-empty lune

Figure 2.3: Illustrating empty lune of influence test

2.3 Delaunay Triangulation and Variations

Another planar graph that has been used for routing in sensor networks is the Delaunay triangulation. Delaunay triangulation was first proposed by Boris Delaunay in 1934 [1]. The Delaunay triangulation of a set of point sites $\{p_0, p_1, p_2, \ldots, p_{n-1}\}$ is the triangulation such that no circumscribing circle of any triangle in the triangulation contains any other point site.

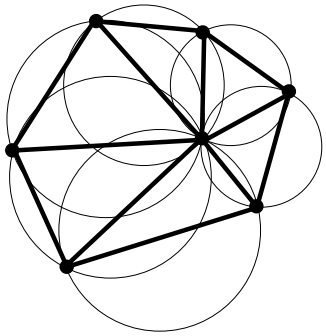

Figure 2.4: Illustrating Delaunay Triangulation

Figure 2.4 shows the Delaunay triangulation of 7 point sites. We can see that circumscribing circles of each triangle contain no point sites. Empty circle property is elaborately illustrated in Figure 2.5.

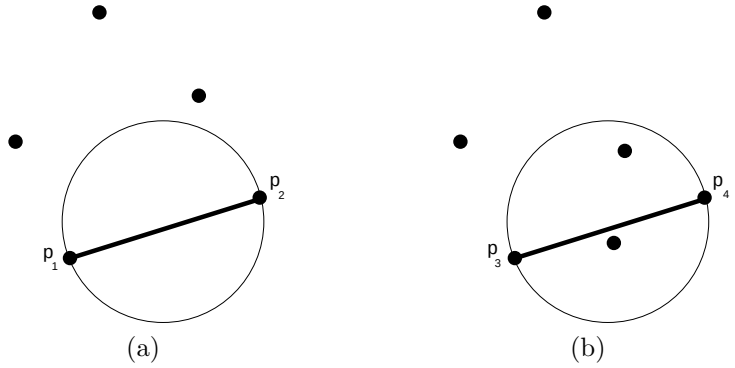

Figure 2.5: Illustrating Empty Circle in Delaunay Triangulation

Figure 2.5 demonstrates an empty circle test on two end points of an edge. In Figure 2.5(a), we can see that there is an empty circle through p_1 and p_2 and hence it is a Delaunay edge. On the other hand, any triangle through p_3 and p_4 can never be made empty and hence the edge connecting p_3 and p_4 is not a Delaunay edge.

Delaunay triangulation is closely related to the structure known as Voronoi Diagram [4]. In fact it is known that Delaunay triangulation is the dual of Voronoi diagram. Many algorithms have been reported to compute Delaunay triangulation [1]. Since Voronoi diagram is the dual of Delaunay triangulation, algorithms for computing Voronoi diagram can be used for obtaining Delaunay triangulation and vice versa [12]. The most popular algorithm for computing Delaunay triangulation is the sweepline algorithm proposed by Fortune [7] which runs in O($nlogn$) time. It is remarked that the problem of computing Delaunay triangulation has a lower bound of $\Omega(nlogn)$ in the comparison tree model of computation [3]. Hence, Fortunes algorithm is also the optimum algorithm. In the context of routing in sensor networks, locally computable structures are highly suitable. Unfortunately Delaunay triangulation can not be computed locally. However, a super-set of Delaunay triangulation briefly described in the next subsection can be computed locally.

2.3.1 Restricted Delaunay Graph(RDG)

Consider a set of point sites S=$\{p_0, p_1, p_2, \ldots, p_{n-1}\}$ in the plane. Each point site corresponds to the position of a sensor node with radio transmission range r=1. (All sensor nodes have identical transmission range.) Suppose each node p_i computes the Delaunay triangulation of p_i and its one hop neighbor. Let T(p_i) denote the Delaunay triangulation of p_i and its one hop neighbors N(p_i). The triangulation T(p_i) is called the local Delaunay triangulation of p_i. The network obtained by the union of all T(p_i)'s is not necessarily planar and it may not be even a triangulation graph. Let G_u denote the union of all T(p_i) for all p_i in S. The graph G_u is not necessarily planar and may not contain all Global Delaunay edges of S. A method of extracting a planar graph from G_u with 1-hop information exchange was proposed by Gao et al. [9]. Such a graph is called Restricted Delaunay Graph(RDG).

A technique to obtain RDG G_r from G_u is to remove *selected crossing edges* (*sr edges*) from G_u [9]. The approach is to check the consistency of edges in the Delaunay triangulation of two neighbor nodes. To understand this method, consider four nodes p_1,p_2,p_3,p_4 as shown in Figure 2.6, where the single triangle is the Delaunay triangulation T(p_1) of 1-hop neighbors N(p_1) and p_1 itself. On the other hand, the Delaunay triangulation T(p_2) of N(p_2) and p_2 is shown in Figure 2.6b. The overlay of T(p_1) and T(p_2) is shown in Figure 2.6c, where two edges cross making T(p_1) $\cup$ T(p_2) non-planar.

Among the crossing pair of edges $\overline{p_1p_3}$ and $\overline{p_2p_4}$, we need to remove one to make T(p_1) $\cup$ T(p_2) planar. The one that is not present in both is removed. The *sr* edge so identified is not a global Delaunay edge. After removing *sr*-edge, we obtain the RDG G_r of four nodes shown in Figure 2.6d. Although the RDG shown in Figure 2.6 is a triangulation graph, for large number of nodes, it need not be a triangulation. Furthermore G_r may contain some edges that are not present in global Delaunay triangulation.

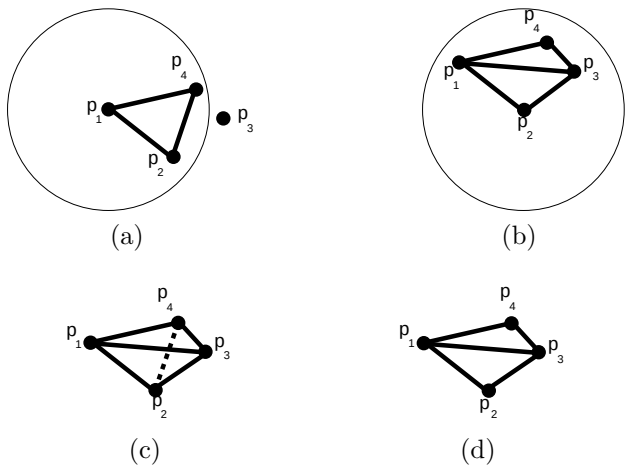

Figure 2.6: Illustrating formation of restricted delaunay graph

A formal local algorithm to construct RDG G_r can be described as follows. Each nodes p_i determines the Delaunay triangulation T(p_i) of p_i and its 1-hop neighbors N(p_i). Each neighbor p_i and p_j exchange T(p_i) and T(p_j). If an edge in T(p_i) is not valid for T(p_j), then that edge is deleted. This local method of removing inconsistency is sketched as Algorithm 4.

Algorithm 4 Algorithm for resolving inconsistency

```
1: E(u):= uv | uv ∈ T(u)
2: for each edge uv in E(u) do
3:    for each edge w in N(u) do
4:       if (u,v ∈ N(w) and uv ∉ T(w)) then
5:          delete uv from E(u)
6:       end if
7:    end for
8: end for
```

2.4 Routing

Routing is the process of selecting a path in a network for sending information from source node to destination node along the network [13]. Routes are constructed in sensor networks using appropriate planar graphs that include Gabriel graphs, relative neighborhood graphs, and restricted Delaunay graphs. In general, if a source node s wants to send a message to a destination node t which is

outside the range of s, then s needs to send the message through a sequence of relay nodes. This sequence of relay nodes together with source and destination nodes define a route connecting s to t. The process of generating these routes is called *routing*. Some of the well known route construction techniques are greedy forward, face routing and hybrid greedy face routing.

2.4.1 Greedy forward routing

Greedy forward routing is a very simple yet one of the most powerful routing algorithms. It constructs route locally in a sequence of steps. In greedy routing, all of the adjacent nodes that are within transmission range are first detected. The next node to forward the message is selected from among the adjacent nodes which are nearer to the target node than the current node. The node that is closest to the target node gets the message. This process is repeated until target is reached.

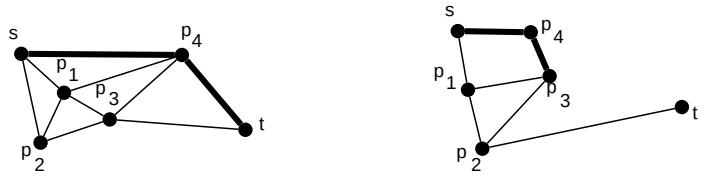

(a) (b)

Figure 2.7: Illustrating Greedy routing

We can illustrate it with a simple example as shown in Figure 2.7(a). Let S=$\{s$, p_1, p_2, p_3, p_4, $t\}$ be the set of nodes where s is the source node and t is the target node. The source node s has three adjacent nodes p_4, p_1 and p_2. Among those three nodes, node p_4 is selected because the distance between $<p_4,t>$ is smaller than $<p_1,t>$ and $<p_2,t>$. Similarly, node p_4 has 4 nodes s, p_1, p_3 and t as adjacent nodes. Since it is directly connected with t, we have found the routing path $s \rightarrow p_4 \rightarrow t$ using greedy forward routing algorithm.

Sometimes, a message gets stuck while using greedy forward routing algorithm. This occurs when the node itself becomes the shortest node rather than its adjacent

nodes. In Figure 2.7(b), we can see that node s finds p_4 as the next node. Similarly, node p_4 finds node p_3 as its next node. Node p_3 has p_4, p_1 and p_2 as its adjacent nodes but none of the nodes have shorter distance than $<p_3,t>$. Hence the message gets stuck at a local minimum.

2.4.2 Face routing

A message delivery method which is guaranteed to work if there is some path connecting source node s to target node t is based on the traversal of the faces of the planar graph formed on the underlying sensor network. A path construction algorithm based on this approach is known as face routing [13]. We can give a brief description of face routing algorithm by considering an example planar graph constructed on the sensor network. The planar graph could be either a Gabriel Graph(GG), or a Relative Neighborhood Graph(RNG) induced by the sensor nodes. In Figure 2.8, a Gabriel graph of eighteen nodes S=$\{s, p_1, p_2, \ldots, p_{15}, p_{16}, t\}$ is shown where there are nine faces that includes the outer unbounded face. Node s and node t are the source node and target node, respectively.

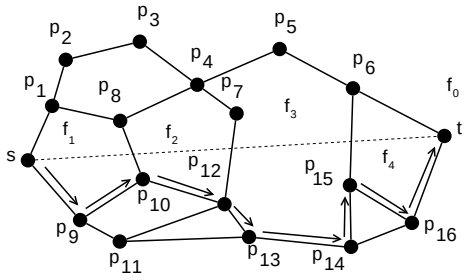

Figure 2.8: Illustrating Face Routing

The source node s knows the position of itself, its 1-hop neighbors, and the position of the target node t. If t is within the transmission range of s, then the message is delivered directly. Otherwise, the algorithm construct the correct face f_c of the Gabriel graph such that (i) s is a node of f_c and (ii) f_c is intersected by the *guiding* line segment $e_g=(\overline{s,t})$. The algorithm determines the *transition edge* e_w of f_c. Transition

edge e_w of f_c is the line segment of f_c that is intersected by the guiding segment e_g. In Figure 2.8,($\overline{p_8, p_{10}}$) is the transition edge. After constructing the current face f_c, the message traverses counterclockwise along the edges of f_c and stops at the transition edge. The message is then delivered to the other face (f_2 in Figure 2.8) incident on the transition edge.

In the next iteration, one of the nodes of the transition edge becomes the source node and the other face incident on e_w becomes the current face f_c. This process of traversing the faces is continued until the target node t is discovered to deliver the message. In Figure 2.8, the constructed route is shown by directed segments.

Algorithm 5 Algorithm for face routing

```
1: p ← s
2: repeat
3:    let f be the face of G with p on its boundary that intersects (p,t)
4:    traverse f until reaching an edge (u,v) that intersects (p,t) at some point p′ ≠
      p
5:    p ← p′
6: until p=t
```

2.4.3 Hybrid greedy face routing

This is a combination of greedy forward routing and face routing. Greedy forward is used as much as possible and when a stuck node is encountered, face routing is used to escape from the stuck node.

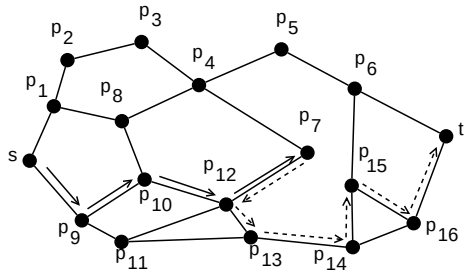

Figure 2.9: Illustrating Hybrid greedy face routing

In Figure 2.9, greedy forward algorithm is used until node gets stuck at node

p_7. Face routing is used to rescue the p_7 node and reach the target.

CHAPTER 3

NODE FILTERING FOR FACE ROUTING

In this chapter, we consider the problem of removing redundant or pseudo-redundant nodes from a set of given nodes. We call this process node filtering.

3.1 Compressing Equivalent Nodes

Consider a set of nodes S= $\{p_0, p_1, p_2, \ldots, p_{n-1}\}$ used for face routing in a sensor network. Two nodes close to each other are called *equivalent* if their transmission ranges cover the same sub-set of nodes. Recall that all nodes are assumed to have an identical transmission range which is taken, without loss of generality, as 1. We can illustrate the notion of *equivalent nodes* with a specific example. In Figure 3.1, the transmission disks of two nodes p_5 and p_6 are shown with dashed circle. This shows that nodes p_5 and p_6 cover the identical set of nodes p_1,p_2,p_3,p_4,p_7 and p_8.

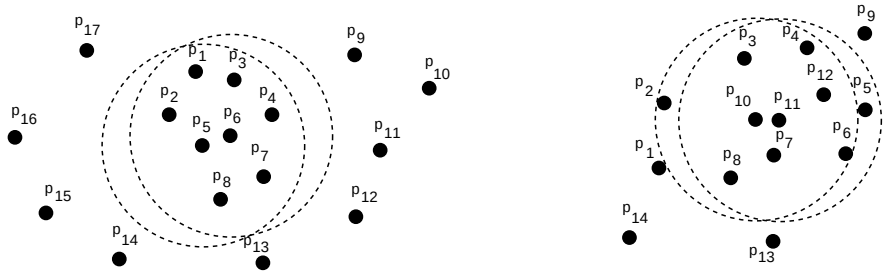

Figure 3.1: Illustrating Equivalent nodes p_5 and p_6

On the right-side of Figure 3.1, two nodes p_{10} and p_{11} are shown which are not equivalent even though they are very close to each other. There can be many nodes equivalent to each other in some rare distributions that contain clustered nodes in some pocket region. This is illustrated in Figure 3.2

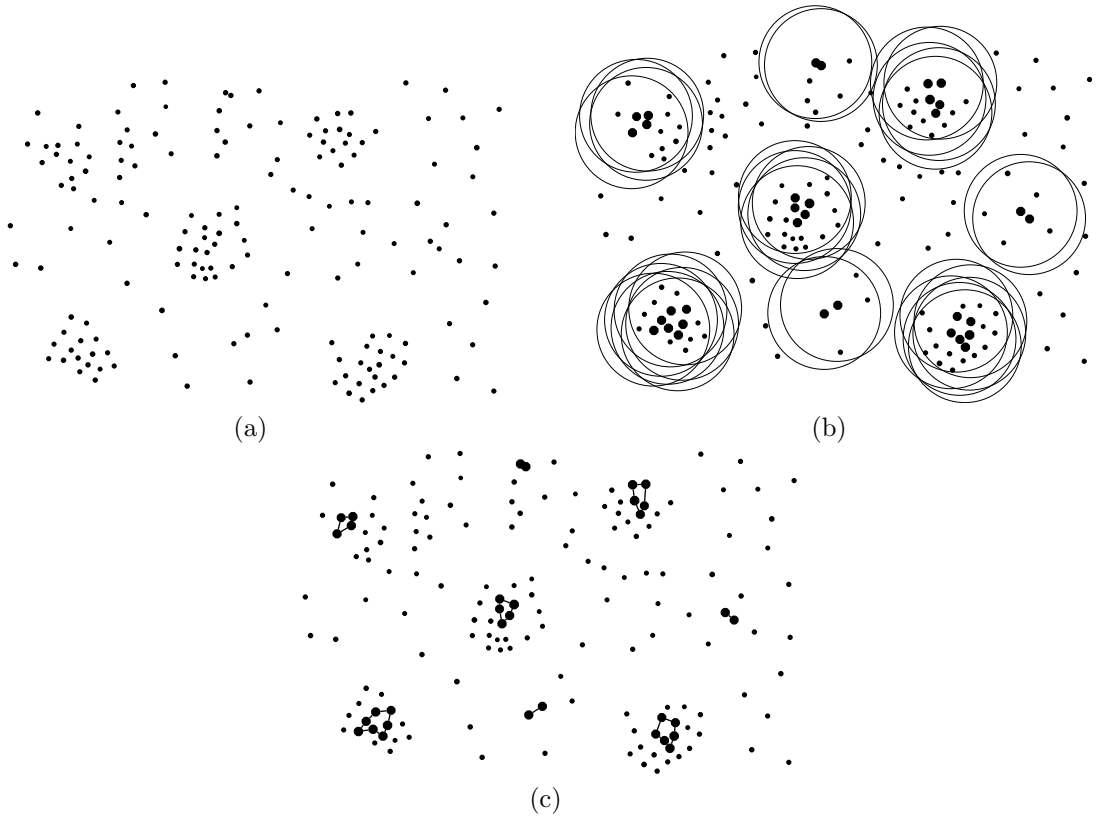

Figure 3.2: Illustrating Clusters of Equivalent nodes

Figure 3.2a is a distribution of sensor nodes where there are five distinctly visible cluster sub-sets of nodes. The clusters that cover identical nodes are highlighted by drawing circles for their range in Figure 3.2b. It is observed in Figure 3.2b that circles in a group cover the same set of nodes.

Definition 3.1.1. (Compressed Gabriel Graph) Consider a Gabriel Graph G(V,E) of a set of sensor nodes. Let C_1,C_2,...,C_k be the set of equivalent nodes in G(V,E). The nodes in V not in the equivalent sets are referred to as *background nodes* and the set of these nodes is denoted by V_B. The set of nodes obtained by adding to V_B exactly one member from each equivalent set is the compressed set of nodes, V_C. The resulting Gabriel graph of V_C, denoted by $G_C(V_C,E_C)$, is the *compressed Gabriel graph*. Figure 3.3 shows the original Gabriel graph and its compressed version for indicated transmission range.

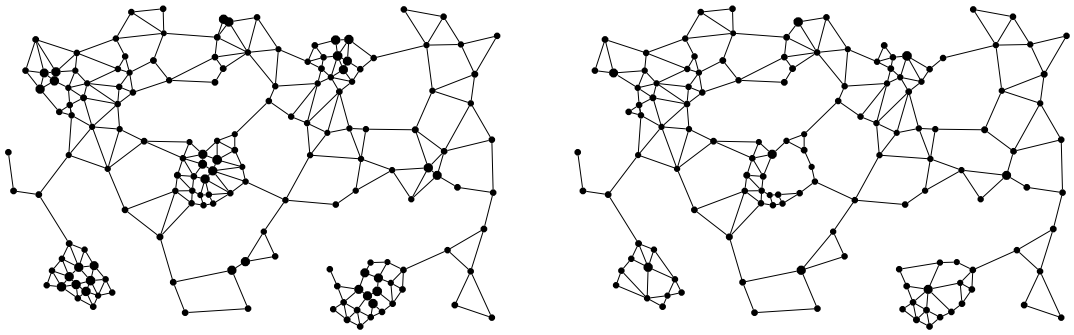

(a) (b)

Figure 3.3: Illustrating Gabriel Graph and its compressed version

Lemma 3.1.1. *If background nodes v_i and v_k are connected in Gabriel graph G(V,E), then they are also connected in the compressed Gabriel graph $G_C(V_C,E_C)$.*

Proof: *Consider any route R connecting node v_i to v_k that passes through a cluster C_j. Let v_e and v_t be the nodes in the background and in R that are closest to the cluster C_j (Figure 3.4).*

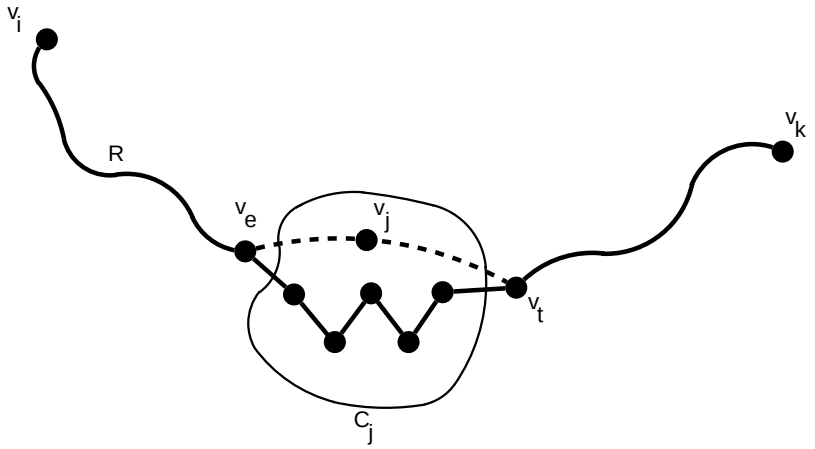

(a)

Figure 3.4: Illustrating a Proof of Lemma 3.1.1

Let v_j be the representative node in C_j. Since v_e and v_t are connected to some nodes in C_j, they are also connected to v_j by the "special path" (v_e,v_j,v_t) shown by dashed segments.

3.2 Solo-Faced Chains

A segment can be viewed to consist of two half-edges. A Gabriel graph in which edges are split into two half-edges is shown in Figure 3.5b. Let $\{e_1,e_2,....,e_{15}\}$ be the edges of a Gabriel graph. The half-edges of e_i are denoted by e_i' and e_i''. Note that e_i' and e_i'' are twin half-edges of each other and they are directed reverse to each other.

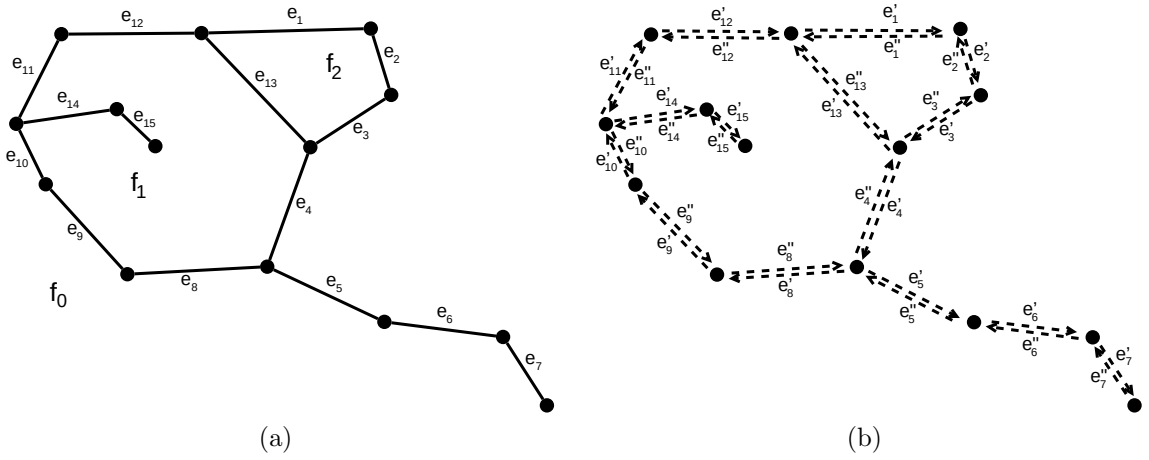

Figure 3.5: Gabriel graph showing edges and its equivalent half edge

Definition 3.2.1. An edge e_i is called *solo-faced edge* if the twin half-edges of e_i i.e. e_i' and e_i'' are incident on the same face. In Figure 3.5a, there are three faces f_0,f_1, and f_2 in the Gabriel graph. Edge e_{15} is a solo-faced edge since e_{15}' and e_{15}'' are incident on the same face f_1. Similarly e_5 is a solo-faced edge as e_5' and e_5'' are incident on the same face f_0. On the other hand, e_4 is not solo-faced as e_4' and e_4'' are incident on faces f_0 and f_1, respectively.

Definition 3.2.2. (Maximal Solo-Faced Chain) A sequence of consecutive solo-faced edges is referred to as a *solo-faced chain*. A solo-faced chain that is not contained in any other solo-faced chain is called a *maximal solo-faced chain*. In Figure 3.5 there are two maximal solo-faced chain which are $e_7e_6e_5$ and $e_{15}e_{14}$. Some Gabriel graphs could have many maximal solo-faced chains. A Gabriel graph with five maximal solo-faced chains is shown in Figure 3.6

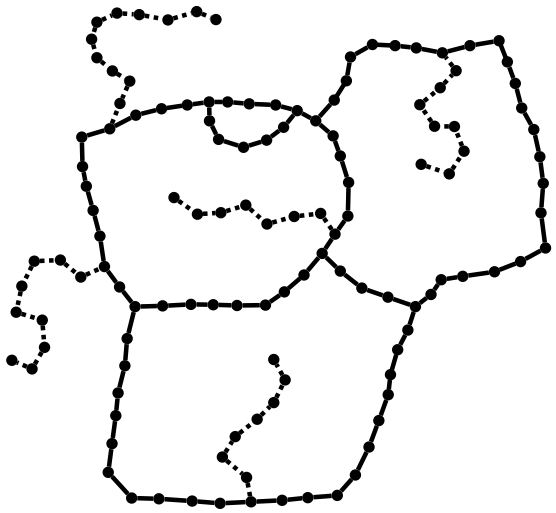

Figure 3.6: Illustrating Solo-Faced Chains

Remark 3.2.1. From now onward, unless otherwise stated, the term *solo-faced chain* will be used to indicate a *maximal solo-faced chain*.

Definition 3.2.3. (Bridge Solo-Faced Chain) Solo-faced chains can be distinguished into two types: Bridge type and Non-Bridge type. If the removal of a solo-faced chain ch_1 from the Gabriel graph breaks the graph into two connected components then ch_1 is called a *bridge solo-faced chain*. In Figure 3.7, there are seven solo-faced chains. Among them only one is a bridge solo-faced chain which is drawn by dashed edges.

Definition 3.2.4. (External Solo-Faced Chains and External Components) Figure 3.8 shows five clusters of nodes A,B,C,D and E. These clusters contain many interconnected nodes and solo-faced chains. Let ch_1,ch_2,ch_3 and ch_4 be the four bridge solo-faced chains connecting these five clusters of nodes. These five clusters of nodes and their bridge solo-faced chains can also be represented in a tree structure as shown in Figure 3.9.

Let s and t be the source and target node present inside clusters A and E respectively. From Figure 3.9, we can see that the actual path to travel from source node to target node is A -> ch_3 -> B -> ch_1 -> E. Only ch_3 and ch_1 are the two bridge solo-faced chains that lie in the path from A to E. All other bridge solo-faced

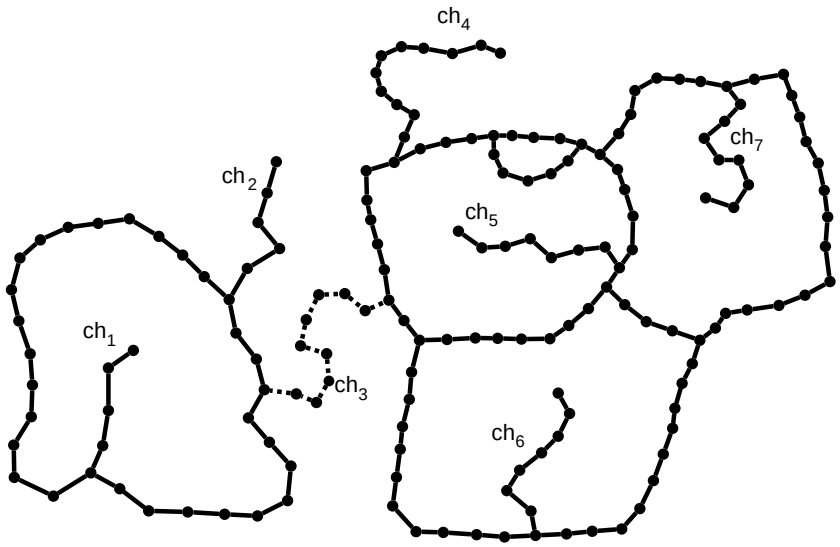

Figure 3.7: Illustrating Bridge Solo-Faced Chain (ch_3-drawn dashed)

chains that don't lie in the path are called external solo-faced chains. There are also clusters of nodes that are not present in the path. These type of cluster of nodes are called external components. In the given figure, two clusters <C,D> and two bridge solo-faced chains <ch_2,ch_4> are called external components and external solo-faced chains respectively.

Figure 3.10 shows the cluster of nodes when non bridge solo-faced chains of Figure 3.8 are removed from the graph. This removal of chains helps in removing unnecessary edges from the graph. The graph can be further optimized by removing external components and external solo-faced chains as shown in Figure 3.11.

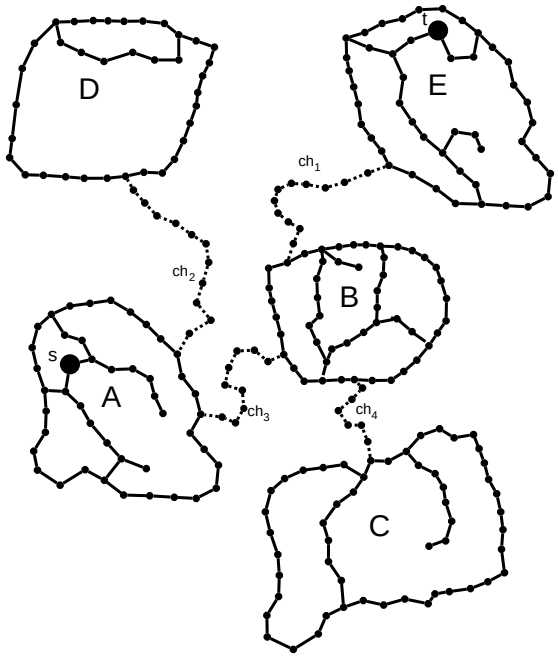

Figure 3.8: Illustrating clusters of nodes connected by Bridge Solo-Faced Chains

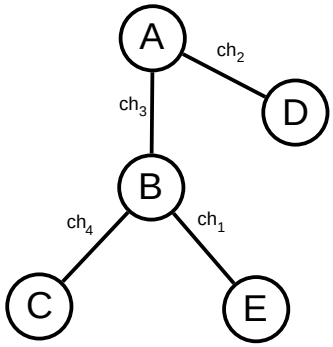

Figure 3.9: Tree representation of Bridge Solo-Faced Chains

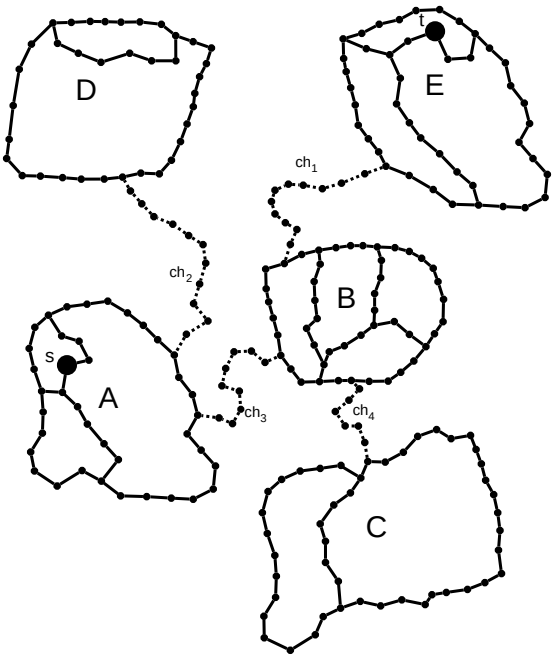

Figure 3.10: Illustrating cluster of nodes without Non Bridge Solo-Faced Chains

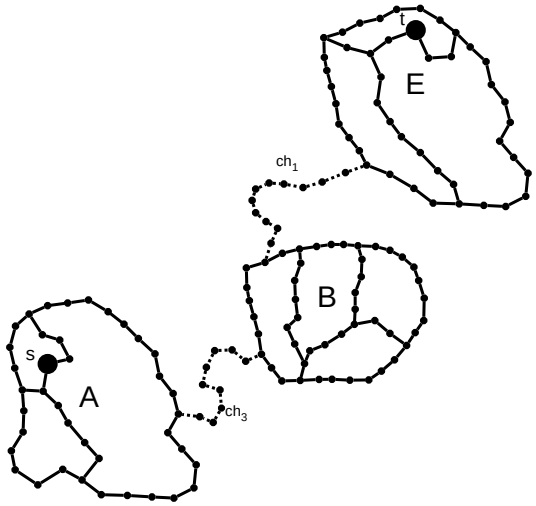

Figure 3.11: Illustrating cluster of nodes after removing External-Components and External Solo-Faced Chains

3.3 Extracting Biconnected Clusters

We could use the depth-first search based on connected component recognition algorithm [14] to extract biconnected clusters. However, a Gabriel graph is a planar graph and a much simpler algorithm can be designed to extract biconnected components. To describe such a simpler algorithm, it is necessary to use the doubly connected edge list (dcel) data structure for representing planar graphs which is described next.

3.3.1 Planar Graph

A graph G(V,E) is called planar if it can be drawn on a plane without intersecting edges.

3.3.2 Planar Straight Line Graph

A planar straight line graph is a planar graph containing all straight edges. They are mostly used to represent maps. Figure 3.12 shows a planar straight line graph containing five vertices and five edges.

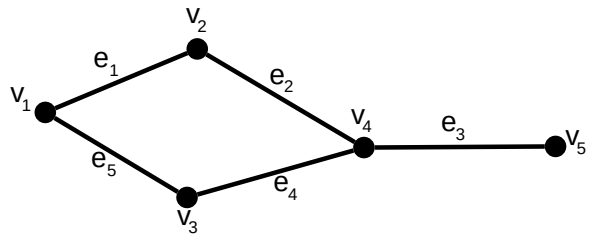

Figure 3.12: Illustrating Planar Straight Line Graph (PSLG)

3.3.3 Doubly Connected Edge List (DCEL)

Double Connected Edge List is a data structure for representing planar straight line graphs. It was originally suggested by Preparata and Muller in 1978 for the representation of 3D convex polyhedra [11]. In DCEL, each edge is viewed as a

pair of twin half-edges pointing in opposite direction. Figure 3.13 shows a doubly connected edge list data structure containing five vertices, ten half edges and two faces.

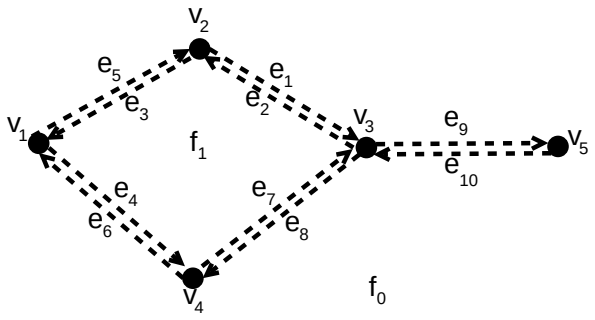

Figure 3.13: Illustrating Doubly Connected Edge List data structure

A DCEL consists of a record for each half edge, face, and vertex. Each half edge record consists of a twin edge, a previous edge, a next edge, an incident face, and a source vertex. The face record consists of a bounding half edge, and each vertex record consists of a incident edge, and its co-ordinate. An example illustrating all the records for each half edge, face and vertex of Figure 3.13 is shown in Table 3.1, 3.2 and 3.3 respectively.

Half Edge	**Twin**	**Prev**	**Next**	**Incident Face**	**Source Vertex**
e_1	e_2	e_5	e_9	f_0	v_2
e_2	e_1	e_7	e_3	f_1	v_3
e_3	e_5	e_2	e_4	f_1	v_2
e_4	e_6	e_3	e_7	f_1	v_1
e_5	e_3	e_6	e_1	f_0	v_1
e_6	e_4	e_8	e_5	f_0	v_4
e_7	e_8	e_4	e_2	f_1	v_4
e_8	e_7	e_{10}	e_6	f_0	v_3
e_9	e_{10}	e_1	e_{10}	f_0	v_3
e_{10}	e_9	e_9	e_8	f_0	v_5

Table 3.1: Record for each half-edge

Face	Bounding Half Edge
f_0	e_9
f_1	e_7

Table 3.2: Record for each face

Node	Incident Edge	Co-ordinate
v_1	e_5	x_1,y_1
v_2	e_3	x_2,y_2
v_3	e_2	x_3,y_3
v_4	e_7	x_4,y_4
v_5	e_{10}	x_5,y_5

Table 3.3: Record for each Vertex

3.3.4 Degree of Vertices

The degree of vertex v is defined as the total number of edges incident to that vertex. Let V=$\{v_1,v_2,v_3,v_4,v_5,v_6\}$ be the total vertices and E=$\{e_1,e_2,e_3,e_4,e_5\}$ be the total edges present in a graph G(V,E) as shown in Figure 3.14(a). Vertex v_3 has degree three because three edges are incident to it. Similarly, vertex v_6 and v_5 have degree one and two respectively. Figure 3.14(b) shows the edges split into two half edges for representing it in a *Doubly Connected Edge List* data structure. An algorithm to detect vertices of degree one is described in algorithm 6.

Algorithm 6 Detect vertices of degree one

```
1: if v_i.getIncidentEdge().getTwin().getNext()==v_i.getIncidentEdge() then
2:     return true.
3: else
4:     return false.
5: end if
```

3.3.5 Removal of Floating Chains

Floating chains have at least one vertex with degree one. Figure 3.15 shows a floating chain e_3,e_4,e_5. In this chain, vertex v_6 has degree one and hence this node

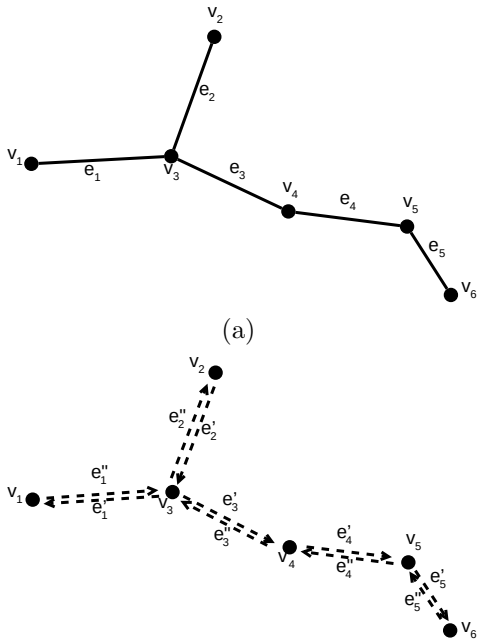

Figure 3.14: Graph showing edges and its equivalent half edge

is removed from the graph. After the removal of vertex v_6 and edge e_5, vertex v_5 becomes another node with degree one. These nodes are removed from the graph one after another until we don't find any vertex with degree one. We also need to consider if the vertex node is the source or target because these nodes shouldn't be removed from the graph. The concept of doubly connected edge list data structure is used to remove floating chains from the graph as shown in Figure 3.15(b).

Algorithm 7 Removing Floating chain

Vertex v_1,v_c
HalfEdge e_1,e_2
$v_c \leftarrow v_i$
while $v_c \neq s \ \ or \ \ t \ \ and \ \ deg(v_c) == 1$ **do**
    $v_1 \leftarrow v_c$
    $e_1 \leftarrow v_1.getIncidentHalfEdge()$
    $e_2 \leftarrow e_1.getTwin()$
    $v_c \leftarrow e_2.getStartNode()$
    $e_2.getPrev().setNext(e_1.getNext())$
    $v_c.setIncidentHalfEdge(e_1.getNext())$
    remove v_1, e_1, e_2 from the graph
end while

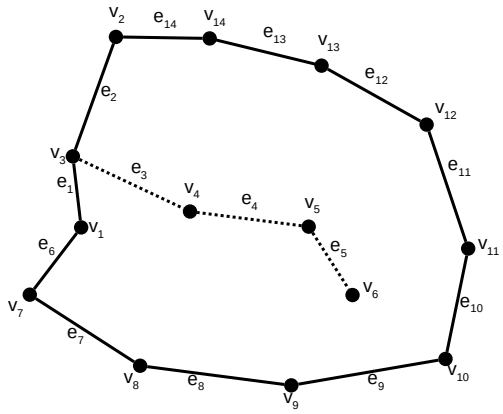

(a)

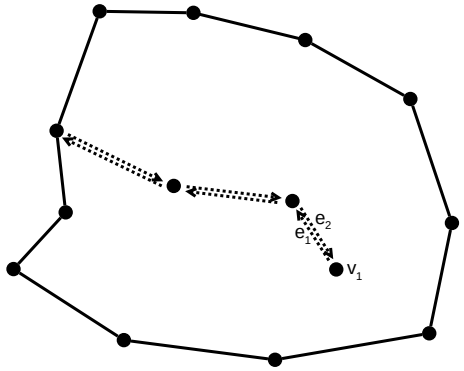

(b)

Figure 3.15: Graph showing floating chains.

We assume that the given Gabriel graph G(V,E) contains no floating chain. If there are floating chains, then we can use Algorithm 7 in Section 3.3.5 to remove them.

A graph G(V,E) is called biconnected if there are two distinct paths between any pair of vertices in G(V,E). A biconnected graph remains connected even if some of its vertices are removed. Figure 3.16(a) is a biconnected graph because any two pair of vertices have at least two distinct paths. Figure 3.16(b) is not a biconnected graph because vertex v_1 and v_4 doesn't have two distinct paths.

In a connected Gabriel graph G(V,E) without floating chains, there could be many biconnected components and bridge chains as shown in Figure 3.17. A dcel representation of G(V,E) is shown in Figure 3.18.

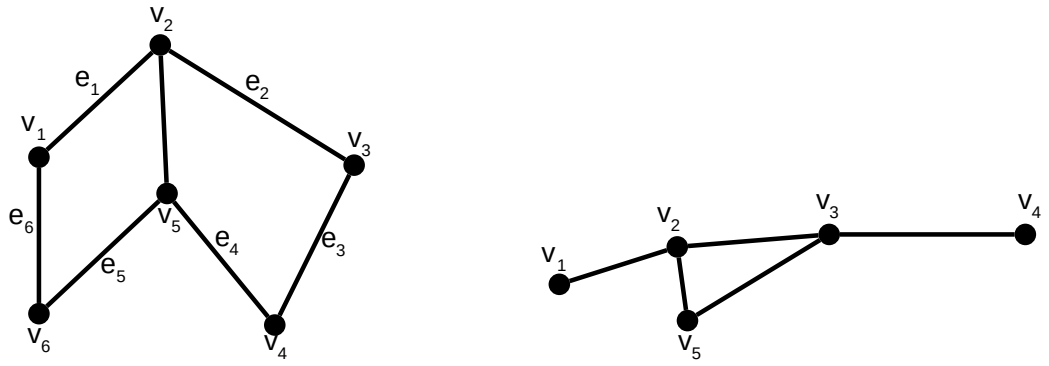

(a) (b)

Figure 3.16: Illustrating biconnected graph

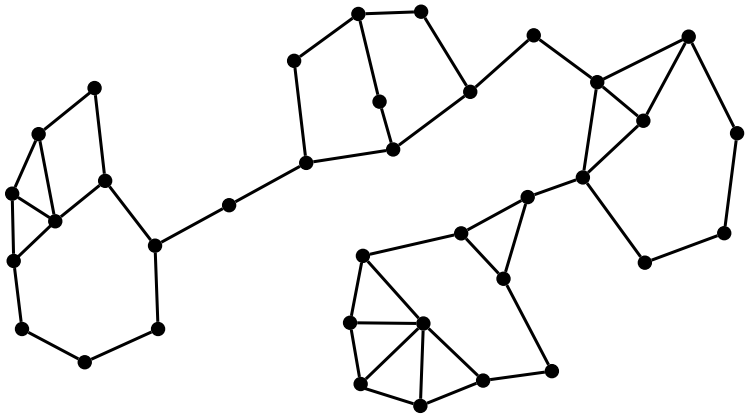

(a)

Figure 3.17: Illustrating biconnected components and bridge chains

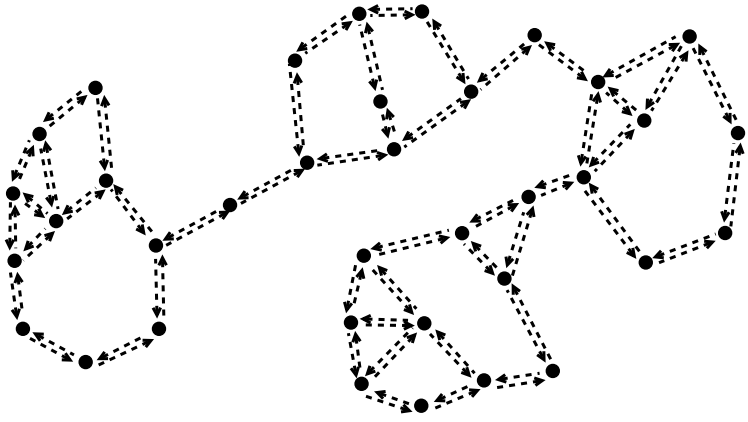

(a)

Figure 3.18: DCEL representation of biconnected components and bridge chains

Definition 3.3.1. A half-edge e_i is called a *transition half-edge* if it satisfies the following conditions.

i) Half-edge e_i is in a bridge-chain.

ii) Let e_j=e_i.next.twin, then e_j.face is not same as e_i.face or e_j.face is not main face (outer unbounded face)

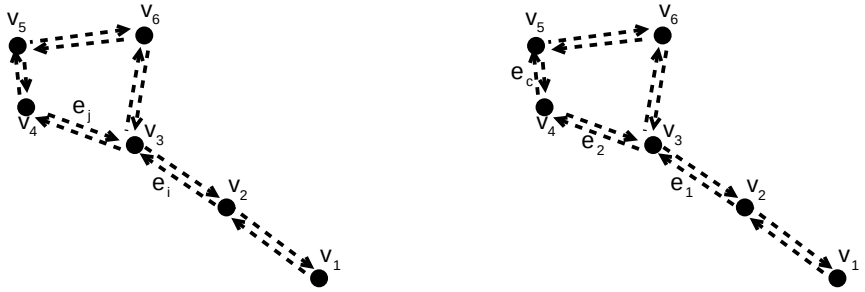

Figure 3.19: Illustrating transition half-edge

Algorithm 8 describes an algorithm to determine transition half edges. This transition half edge algorithm is used for finding bi-connected graphs in Algorithm 9. The three half-edges e_1, e_2, and e_c of Algorithm 9 is shown in Figure 3.19(b). Algorithm 10 describes the procedure to remove external components and external solo-faced chains from the graph.

Algorithm 8 Find all Transition Half Edge

```
1: for each edge e_i in bridge solo-faced chain do
2:    if e_i.getNext().getTwin().hasMainFace()==false then
3:       add e_i to transition edge list
4:    end if
5: end for
```

Algorithm 9 Find Bi-Connected graph from transition edge

transition edge e_i
half edge e_1,e_2,e_c
$e_1 \leftarrow e_i$
$e_2 \leftarrow e_1.getNext()$
if e_2.getNext().getTwin().hasMainFace()==true **then**
    e_c=e_2.getNext().getTwin().getNext()
else
    e_c=e_2.getNext()
end if
Edgelist e_l
e_l.add(e_2)
while $e_c \neq e_2$ **do**
    e_l.add(e_c)
    if e_c.getNext().getTwin().hasMainFace()==true **then**
        e_c=e_c.getNext().getTwin().getNext()
    else
        e_c=e_c.getNext()
    end if
end while
create a polygon p using all the edges of edge list e_l
for each edge $e1_i$ present in graph **do**
    if $e1_i$ is present inside p **then**
        e_l.add($e1_i$)
    end if
end for
output e_l as total edges of one bi-connected graph obtained from transition edge e_i

Algorithm 10 Remove External Solo-Faced Chains and External Components from graph

label each edge of a bi-connected graph by a tree.
use transition half-edge to find connection between two trees
find the tree present in source and target
use depth first search to find the path from source to target.
delete all bridge solo-faced chains that don't lie in the path
delete all vertices and edges that don't have trees that lie in the path.

CHAPTER 4

IMPLEMENTATION

This chapter describes the implementation of node filtering and face routing in sensor networks. All the programs are implemented in Java. The program is divided into three projects.

The first project shows the implementation of Gabriel Graph, Relative Neighborhood Graph and Unit Disk Graph. These graphs are implemented for some randomly generated nodes. It also shows how a node routes a path from source node to target node using Greedy Routing, Face Routing and Hybrid Routing.

The second project deals with filtering of nodes in a network. This project mainly focuses on equivalent nodes, solo-faced chains and external components. It shows the difference in a network before and after removal of equivalent nodes. It also shows how the network is changed when nodes present on solo-faced chains and external components are removed from the graph.

The third project is the combination of first and second project. This project shows how the node routes a path from source node to target node using different routing algorithms and the difference found when equivalent nodes, solo-faced chains and external components are removed from the graph.

4.1 Introduction to Java

Java is a programming language developed by James Gosling [2] at Sun Microsystems. It is a high-level object-oriented programming language. Java derived much of its syntax from C and C++. Its applications are typically compiled to bytecode that can run on any Java Virtual Machine(JVM) regardless of computer architecture. It is intended to let application developers write once, run anywhere

(WORA) [5], meaning that code that runs on one platform does not need to be recompiled to run on another.

4.2 Interface Description

4.2.1 Project 1

Figure 4.1 shows the main user interface of project 1. It is drawn by extending the JFrame class. It consists of a menu bar, a drawing panel, a right panel and a bottom panel.

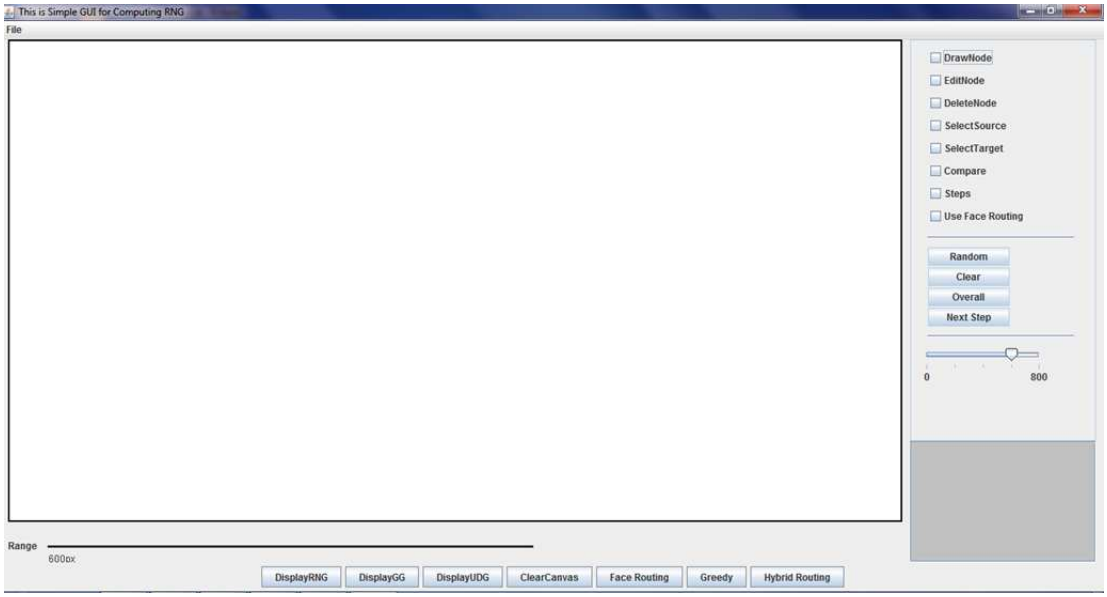

Figure 4.1: Illustrating User Interface of Project 1

The menu bar consists of a File Menu which contains 4 menu items *Open*, *Save*, *Export* and *Exit*. The *Open* Menu Item is used for opening a saved file and *Save* Menu Item is used for saving the graph. Similarly, *Export* Menu Item is used to export the file to XFig format and *Exit* Menu Item helps to exit the program.

A big center panel is the drawing panel in which all nodes are drawn. It shows all the graphic output of the program.

A right panel consists of eight checkboxes. The first checkbox is *DrawNode*. This checkbox helps in drawing nodes on the drawing panel. A user can check this checkbox

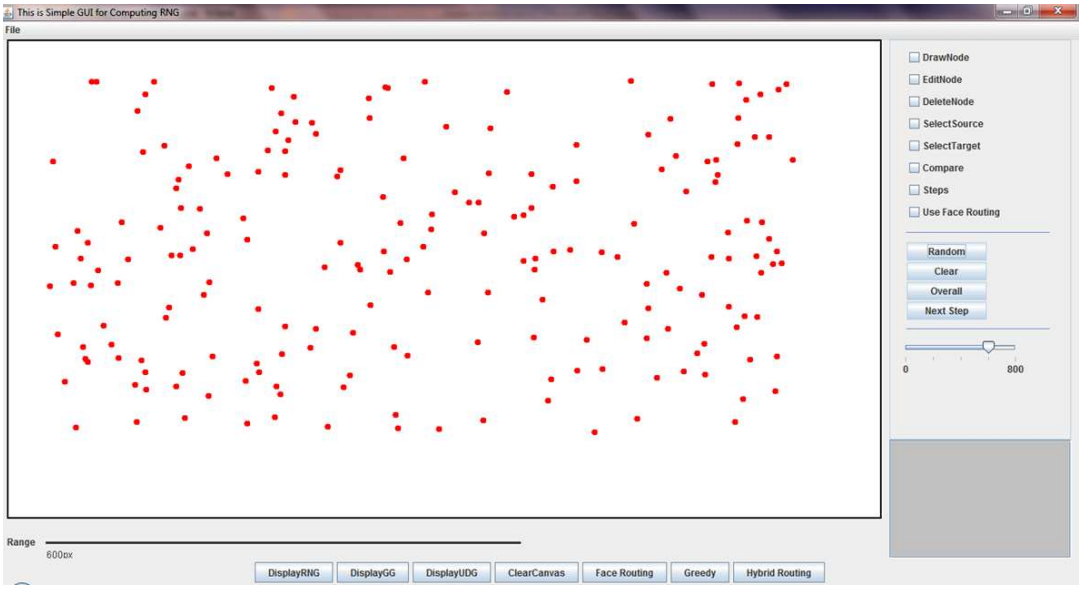

Figure 4.2: Illustrating Random Nodes

and draw nodes on the drawing panel using mouse. *EditNode* and *DeleteNode* checkboxes are used for editing and deleting nodes respectively. If we select the *SelectSource* checkbox and select any node, the node becomes the source. Similarly, we can select the Target node by selecting the $TargetNode$ check box. The next check box is *Compare* which helps to compare the graphs. If this check box is selected and we try to draw a Gabriel Graph, it opens a new Frame containing Gabriel Graph and Unit Disk Graph. *Steps* checkbox helps in displaying steps of routing. The last checkbox is $UseFaceRouting$ which helps on using the face routing when nodes get stuck during greedy routing.

A right panel also contains four buttons *Random*, *Clear*, *Overall*, and $NextStep$. *Random* button helps in displaying random nodes. These nodes can be cleared by using *Clear* button. *Overall* Button helps in comparing the path travelled by Greedy and Face Routing on RNG and GG. $NextStep$ button is used to display the next step in routing. There is also a range slider to change the range of sensor nodes.

Finally, there is a bottom panel containing seven buttons. $DisplayRNG$, $DisplayGG$ and $DisplayUDG$ buttons are used to display Relative neighborhood

graph, Gabriel graph and Unit disk graph respectively. *ClearCanvas* button is used to clear the graph. *FaceRouting*, *Greedy* and *HybridRouting* are the three routing buttons to demonstrate the routing operations.

Figure 4.2 shows a few red random nodes drawn on the user interface. It is drawn by clicking *Random* button. We can also add nodes to it by selecting *DrawNode* checkbox. The Gabriel Graph of the above nodes is shown in Figure 4.3. It also shows the source and target nodes. The greedy routing path taken from source node to target node is illustrated in Figure 4.4.

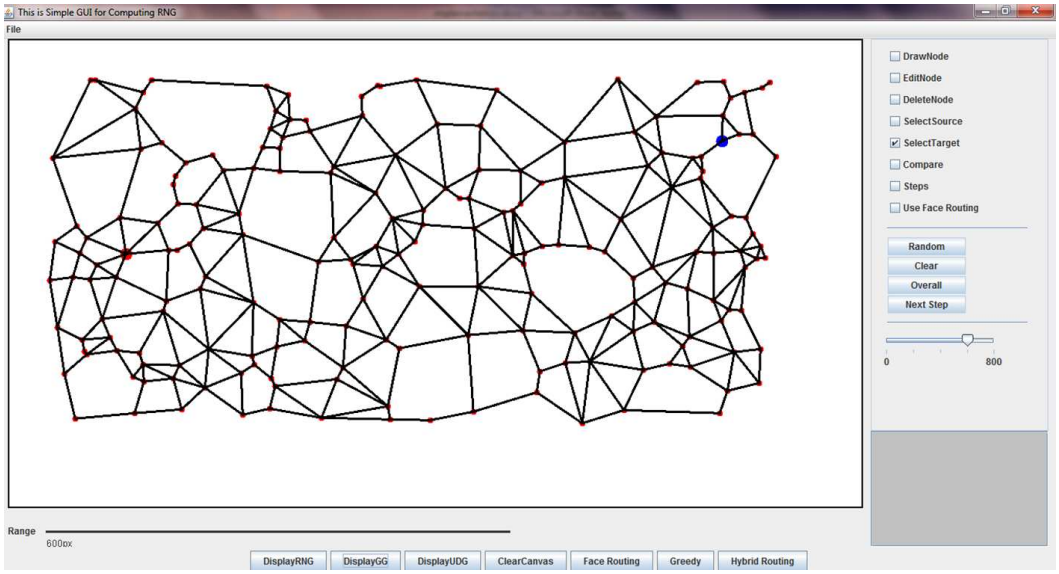

Figure 4.3: Illustrating Gabriel Graph containing source and target nodes

4.2.2 Project 2

The user interface of project 2 is similar to project 1. Figure 4.5 illustrates the user interface of Project 2. It consists of menu bar, drawing panel, range panel and checkboxes. The menu bar consists of a File Menu which contains 3 menu items *Open*, *Save* and *Exit* which are similar to Project 1.

The big white panel is a drawing panel where nodes are drawn. The buttom panel contains a range panel which helps in changing the range of sensor nodes.

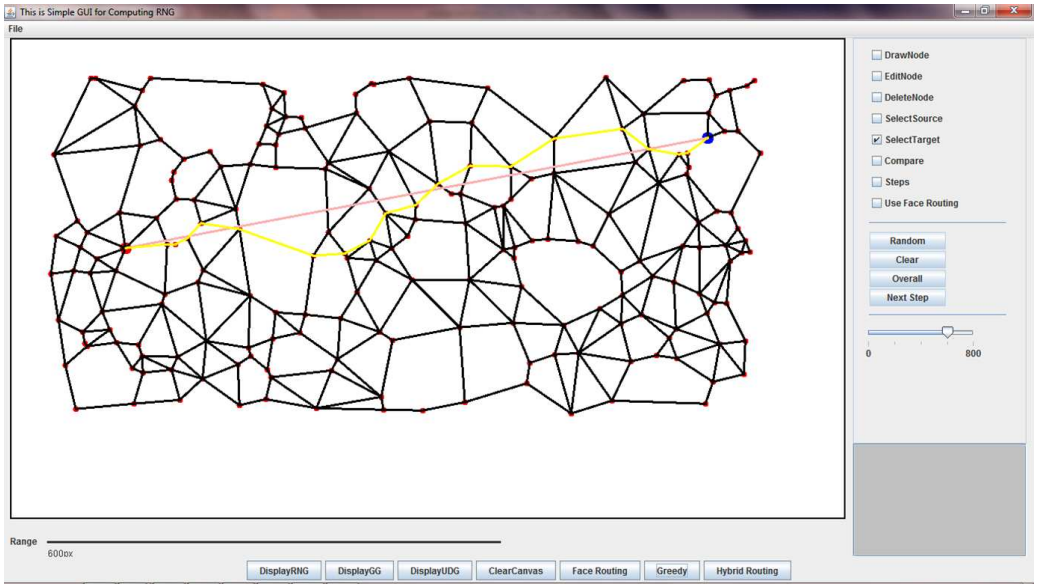

Figure 4.4: Illustrating the routing path taken from source node to target node

The right panel consists of many checkboxes. There are five checkboxes present at the top of right node. They are *DrawNode*, *EditNode*, *DeleteNode*, *DisplayGG* and *Displayrange*. The top three checkboxes are used for drawing, editing and deleting nodes. The *DisplayGG* check box helps in displaying the Gabriel graph of nodes. The Display range checkbox helps in displaying the range of sensor nodes.

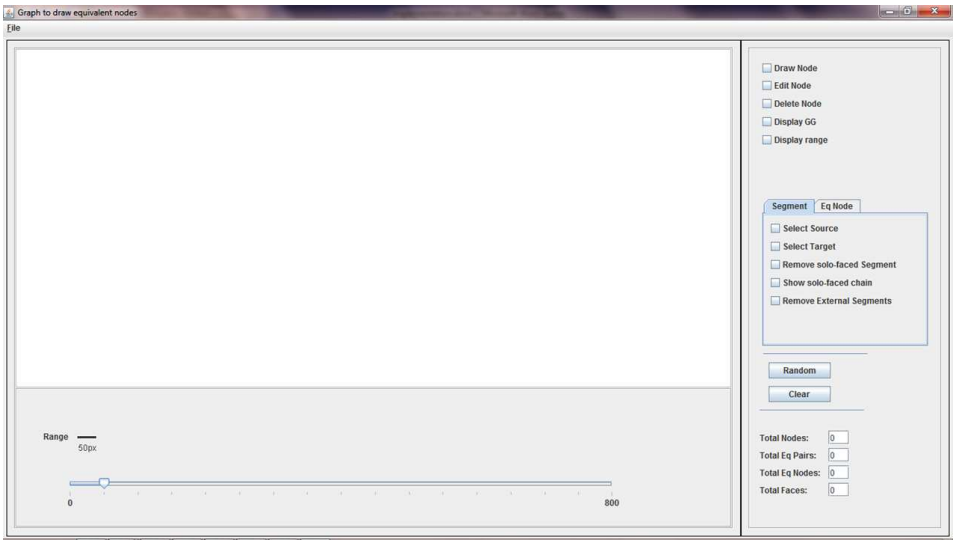

Figure 4.5: Illustrating the user interface of Project 2

There are two tabs, *Segment* and *EqNode*. The Segment tab contains five

checkboxes. The first two checkboxes are used to select source and target. The third and fourth checkboxes are used to remove and show solo-faced segments respectively. The last checkbox is used to remove external segments present on the graph. The graph showing solo-faced segments is illustrated in Figure 4.6. Figure 4.8 shows a graph when external segments are removed from Figure 4.7.

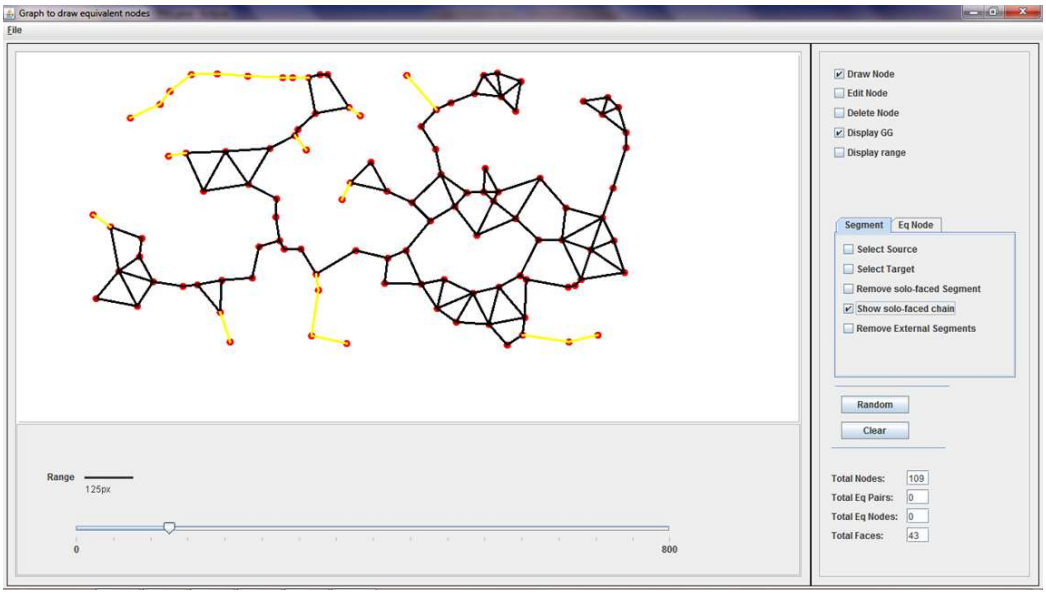

Figure 4.6: Illustrating solo-faced chains

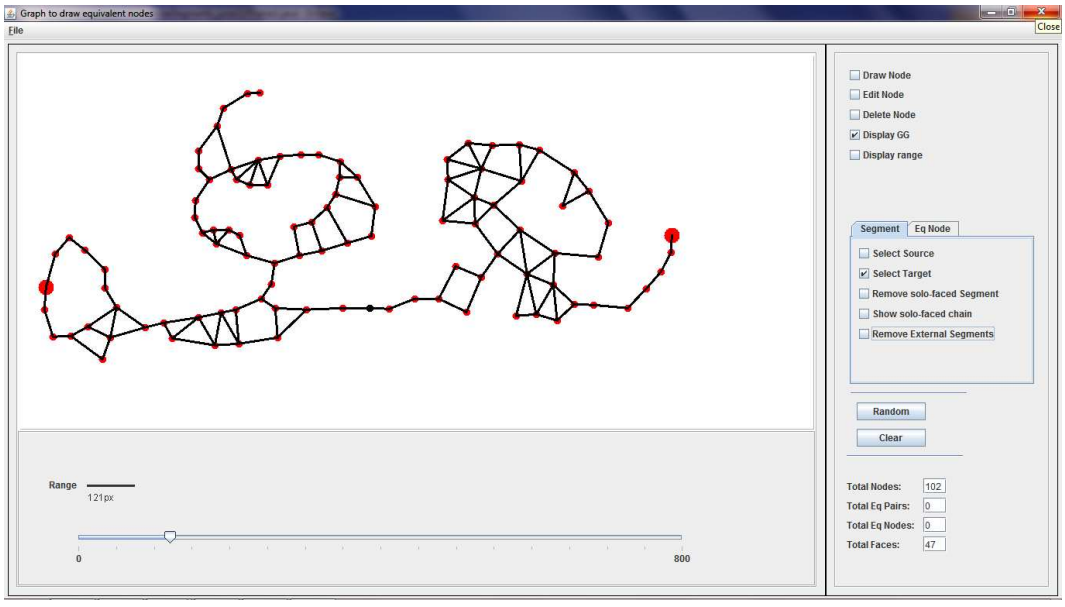

Figure 4.7: Illustrating graph containing external segments

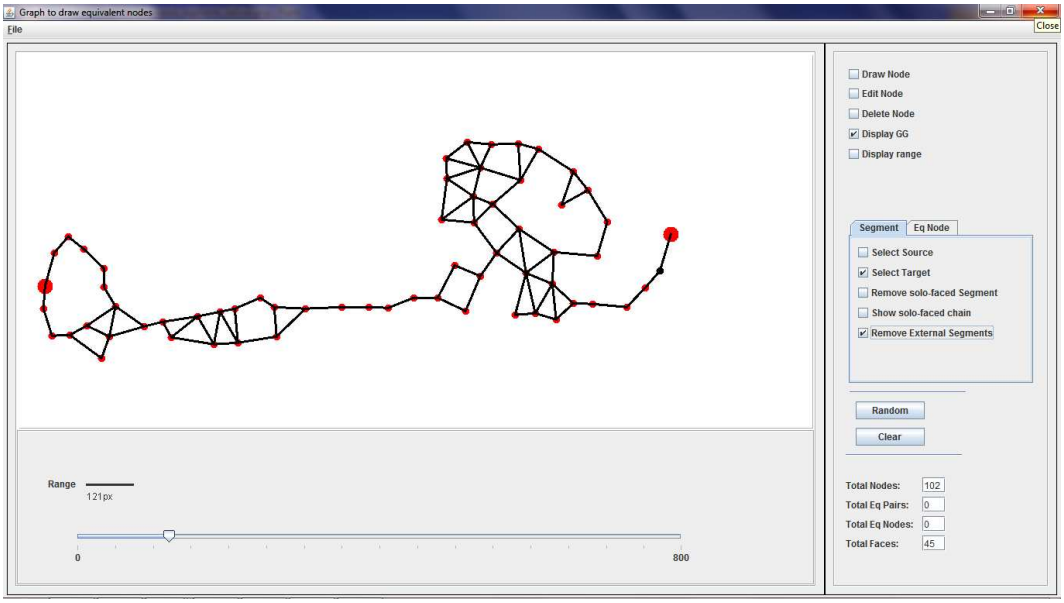

Figure 4.8: Illustrating graph after removal of external segments

EqNode tab contains 3 checkboxes. The first checkbox is used to show only one equivalent node among all equivalent nodes. The second checkbox displays only one equivalent node picked randomly. The third checkbox is used to display equivalent nodes. A graph illustrating equivalent nodes is shown in Figure 4.9. There are also two buttons, *Random* and *Clear* which generates and clears all nodes respectively.

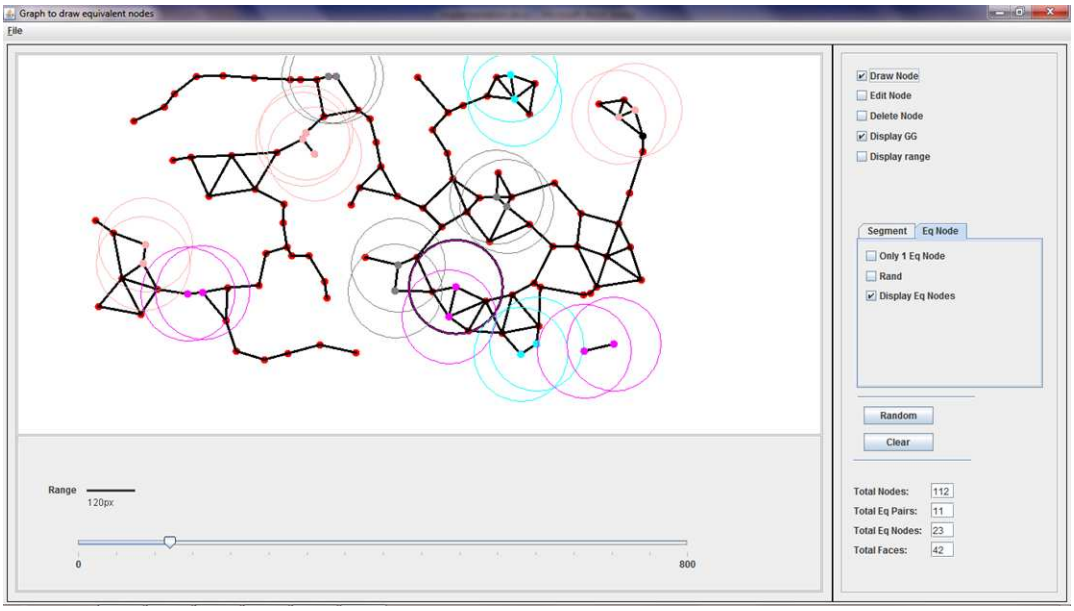

Figure 4.9: Illustrating equivalent nodes

4.2.3 Project 3

The user interface of project 3 consists of a menu bar, drawing panel and right panel. The menu bar consists of three menu items, *open*, *save* and *exit*. The drawing panel is used for drawing the graph.

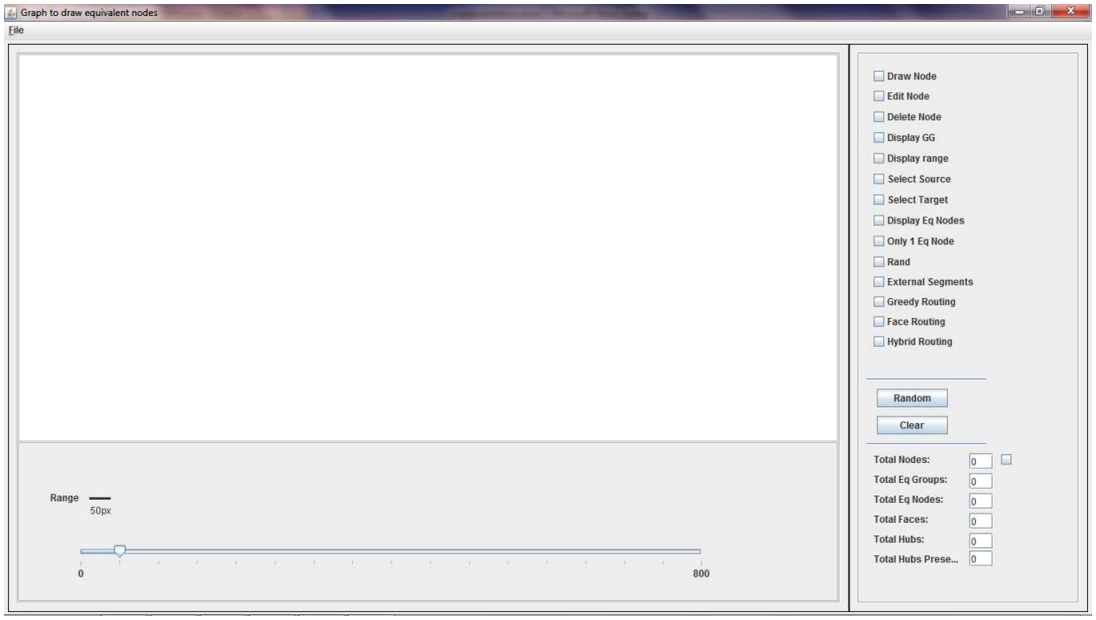

Figure 4.10: Illustrating user interface of project 3

The right panel consists of 15 checkboxes. The first three checkboxes, $DrawNode$, $EditNode$ and $DeleteNode$ are used to draw, edit and delete nodes present on graph. $DisplayGG$ checkbox helps in displaying the Gabriel Graph of nodes. $DisplayRange$ checkbox is used to display range of each sensor nodes.

There are 2 other checkboxes, $SelectSource$ and $SelectTarget$, to select source and target nodes. $DisplayEq.Nodes$ and $Only1Eq.Node$ checkboxes are used to display equivalent nodes and only one equivalent nodes respectively. The *rand* checkbox is used for selecting only one equivalent node in random from clusters of equivalent nodes.

The $ExternalSegment$ checkbox is used to show only external segments obtained after removing equivalent nodes, solo-faced chains and external components.

Finally, there are three routing checkboxes, $GreedyRouting$, $FaceRouting$ and

HybridRouting, to show how the path is traced when these routing algorithms are used.

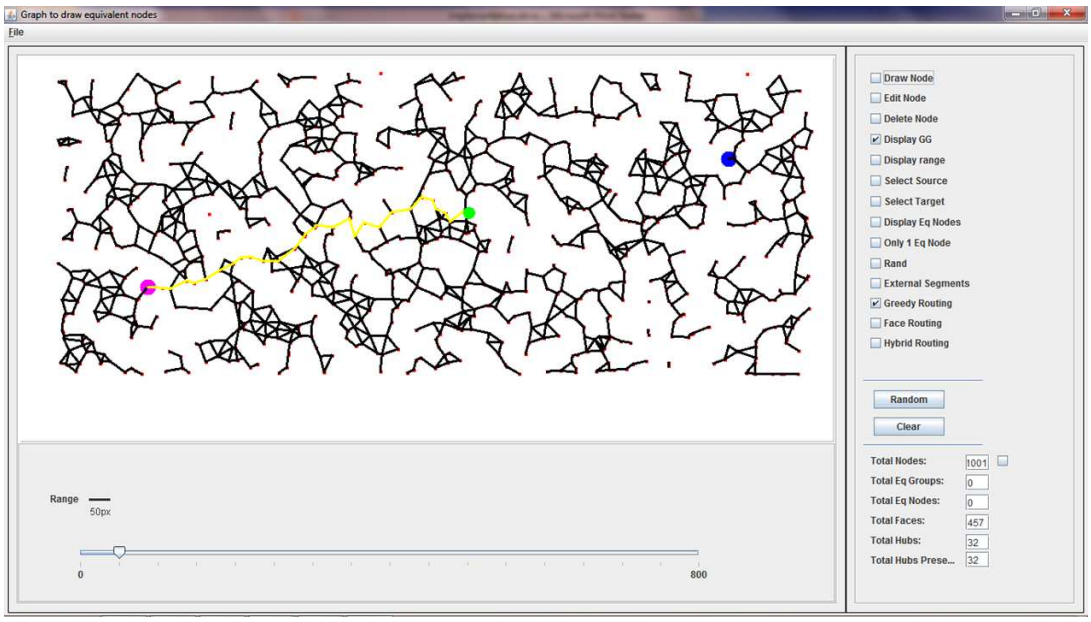

Figure 4.11: Illustrating greedy routing traced by nodes

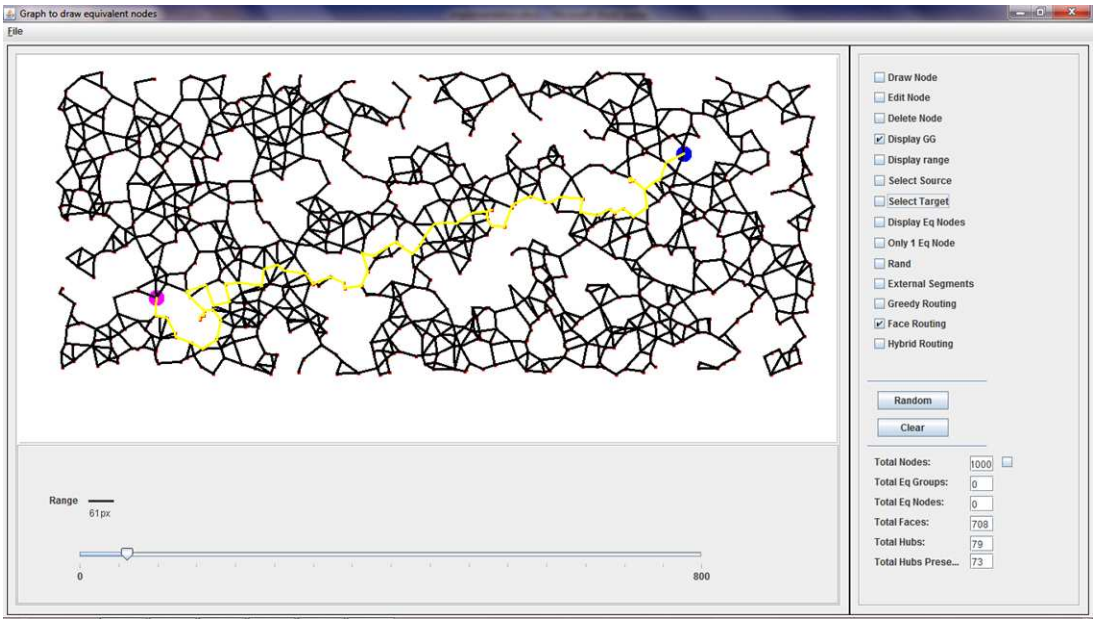

Figure 4.12: Illustrating face routing traced by nodes

In Figure 4.11, we can see the path traced when we apply the greedy routing algorithm. We can also see that the node got stuck while using greedy routing.

Figure 4.12 shows the path traced when we applied the face routing algorithm.

The rightmost bottom textboxes are used for getting information from the graph. It provides information regarding total nodes, total equivalent nodes and total equivalent groups. It also provides information regarding total faces and total hubs as illustrated in Figure 4.12.

4.3 Observation

Table 4.1a and 4.1b shows the random nodes and their respective ranges taken for the experiment. Table 4.1a shows the total nodes and their ranges when they are partially connected and Table 4.1b shows the total nodes when they are completely connected.

Nodes	**Range**
200	104
300	87
400	75
500	66
700	60

(a)

Nodes	**Range**
200	238
300	192
400	156
500	133
600	116

(b)

Table 4.1: Nodes and their range

We drew Gabriel graphs with the above nodes and tested them in different ranges. We found out that the equivalent nodes varied with the range of nodes. Table 4.2a and 4.2b show the results obtained when the graphs were partially and completely connected respectively. The equivalent nodes got reduced by 12.28% when nodes were partially connected. On the other hand, the nodes got reduced by 5.17% when the nodes were completely connected. This shows that equivalent nodes were mostly found when nodes have a small range (partially connected).

We also counted the total hubs used while routing from source node to target node under different routing conditions. We experimented with greedy, face and

Total Nodes	Range	Total Eq. Groups	Total Eq. Nodes	Total Nodes after removing Eq. Nodes	% change
200	104	25	55	170	15
300	87	35	76	259	13.67
400	75	38	85	353	11.75
500	66	55	115	440	12
700	60	54	117	637	9

(a)

Total Nodes	Range	Total Eq. Groups	Total Eq. Nodes	Total Nodes after removing Eq. Nodes	% change
200	238	12	26	186	7
300	192	9	18	291	3
400	156	20	40	380	5
500	133	22	47	475	5
600	116	29	64	565	5.83

(b)

Table 4.2: Total changes in equivalent nodes

hybrid routing and calculated the total hubs present before and after removing equivalent nodes. We also tested it when the external components were removed from the graph. Table 4.3 gives all the details that we calculated when the graph was partially connected. Table 4.3a gives the changes in hubs when we used greedy routing. Similarly, Table 4.3b and 4.3c gives all the details about changes obtained while using face and hybrid routing respectively. We can see that most of the nodes got stuck when we used greedy routing on partially connected graphs. One of the most significant results can be seen on Table 4.3b and 4.3c where the total hubs reduced a lot during face and hybrid routing respectively.

Table 4.4 shows the total change in hubs when different routing algorithms were used before and after removing equivalent nodes and external segments on completely connected graphs. Table 4.4a, 4.4b and 4.4c shows the changes obtained when greedy, face and hybrid routing were used. The table shows that there wasn‘t significant

Total Nodes	Range	Total hubs present		
		Before Removing Eq. Nodes	After Removing Eq. Nodes	After Removing External Segments
200	104	11(S)	11(S)	11(S)
300	87	3(S)	3(S)	3(S)
400	75	0(S)	0(S)	0(S)
500	66	2(S)	2(S)	2(S)
700	60	1(S)	1(S)	1(S)

(a)

Total Nodes	Range	Total hubs present		
		Before Removing Eq. Nodes	After Removing Eq. Nodes	After Removing External Segments
200	104	51	46	42
300	87	782	726	446
400	75	800	713	402
500	66	1044	938	436
700	60	386	350	209

(b)

Total Nodes	Range	Total hubs present		
		Before Removing Eq. Nodes	After Removing Eq. Nodes	After Removing External Segments
200	104	37	32	32
300	87	289	273	165
400	75	180	165	88
500	66	1443	1493	431
700	60	437	389	243

(c)

Table 4.3: Total changes in hubs (partially connected graph)

improvement when the nodes were completely connected.

From Table 4.3 and 4.4, we can see that more redundant nodes were found on partially connected graphs.

Total Nodes	Range	Total hubs present		
		Before Removing Eq. Nodes	After Removing Eq. Nodes	After Removing External Segments
200	238	23	23	23
300	192	27	27	27
400	156	31	31	31
500	133	35	33	33
600	116	31	28	28

(a)

Total Nodes	Range	Total hubs present		
		Before Removing Eq. Nodes	After Removing Eq. Nodes	After Removing External Segments
200	238	35	34	34
300	192	32	32	32
400	156	39	38	38
500	133	42	40	40
600	116	45	39	39

(b)

Total Nodes	Range	Total hubs present		
		Before Removing Eq. Nodes	After Removing Eq. Nodes	After Removing External Segments
200	238	23	23	23
300	192	27	27	27
400	156	31	31	31
500	133	35	33	33
600	116	31	28	28

(c)

Table 4.4: Total changes in hubs (completely connected graph)

CHAPTER 5

CONCLUSION

We presented a comprehensive review of networks used for communication in sensor networks. The reviewed networks included relative neighborhood graphs (RNG), Gabriel graphs (GG), Delaunay triangulation (DT), and restricted Delaunay graphs (RDG). Well-known routing algorithms for message forwarding in sensor networks were also examined. The examined routing algorithms include (i) greedy forward routing (ii) face routing, and (iii) greedy face hybrid routing.

We formulated the notion of redundant nodes in sensor networks. We showed that only one member from a set of equivalent nodes can be retained. This leads to a filtering algorithm for removing most redundant nodes. We proved that the removal of redundant nodes does not affect the connectivity between source node and target node. Another technique presented to filter unnecessary nodes is the removal of solo-faced chains. We also show that for fixed source node s and fixed target node t, some two-connected network components can be removed without compromising the connectivity between s and t.

We presented an experimental study of the proposed algorithms. The proposed algorithms were implemented in Java programming language. The resulting prototype program is easy to use and has a user friendly graphical interface. Observed results show that the proposed algorithms are effective in filtering redundant nodes. In many randomly generated networks, 12.28% of nodes can be identified as redundant.

This study can be pursued further. We studied the filtering problem for a two dimensional network. It would be interesting to extend the proposed algorithm to non-planar networks including three dimensional graphs.

Another avenue for further research would be to examine the performance of the

proposed algorithms for actual sensor networks formed by distributing sensor nodes on the surface of outdoor fields.

REFERENCES

[1] Delaunay triangulation. http://en.wikipedia.org/wiki/Delaunay_triangulation.

[2] Java (programming language). http://en.wikipedia.org/wiki/Java_%28programming_language%29.

[3] A visual implementation of fortune's voronoi algorithm. http://www.diku.dk/hjemmesider/studerende/duff/Fortune/.

[4] Voronoi diagram. http://en.wikipedia.org/wiki/Voronoi_diagram.

[5] What is java, it's history? http://www.roseindia.net/java/beginners/what-is-java.shtml.

[6] Wireless sensor network. http://en.wikipedia.org/wiki/Wireless_sensor_network.

[7] Steven Fortune. A sweepline algorithm for voronoi diagrams. *Algorithmica*, 2:153–174, 1987.

[8] K. R. Gabriel and R. R. Sokal. A new statistical approach to geographic variation analysis. *Systematic Zoology (Society of Systematic Biologists)*, 18:259–270, 1969.

[9] J. Hershberger L. Zhang J. Gao L. J. Guibas and A. Zhu. Geometric spanners for routing in mobile networks. *IEEE Journal on selected areas in communications*, 23:174–185, 2005.

[10] D. W. Matula and R. Sokal. Properties of gabriel graphs relevant to geographic variation research and the clustering of points in the plane. 12:205–222, 1980.

[11] D. E. Muller and F. P. Preparata. Finding the intersection of two convex polyhedra. 7:217–236, 1978.

[12] Joseph OŔourke. *Computational Geometry in C.* Cambridge University Press, 1994.

[13] I. Stojmenovic P. Bose P. Morin and J. Urrutia. Routing with guaranteed delivery in ad hoc wireless networks. pages 609–616, 2001.

[14] R. L. Rivest C. Stein T. H. Cormen, C.E. Leiserson. Introduction to algorithms.

[15] G. T. Toussaint. The relative neighbourhood graph of a finite planar set. 12:261–268, 1980.

[16] F. Zhao and L. Guibas. *Wireless Sensor Networks*. Morgan Kaufmann Publishers, 1994.

VITA

Graduate College
University of Nevada, Las Vegas

Umang Amatya

Home Address:
4441 ESCONDIDO STREET APT 1205
Las Vegas, NV 89119

Degree:
Bachelor of Computer Engineering
Institute of Engineering, Pulchowk Campus, Tribhuvan University, Nepal

Thesis Title: Node Filtering and Face Routing for Sensor Network

Thesis Examination Committee:
Chairperson, Dr. Laxmi P. Gewali, Ph.D.
Committee Member, Dr. John T. Minor, Ph.D.
Committee Member, Dr. Ju-Yeon Jo, Ph.D.
Graduate Faculty Representative, Dr. Rama Venkat, Ph.D.